Field induced slow magnetic relaxation in linear homotrinuclear manganese heterospin coordination compound with S = 7/2 ground state and intriguing spin density distribution

Igor N. Shcherbakov,*[a] Ilya I. Krotkii, [a] Victoria I. Kazachkova, [a] Sergey N. Lyubchenko, [a] Nikolay N. Efimov, [b] Arshak A. Tsaturyan, [c, d] and Vladimir A. Lazarenko[e].

[a.] *Southern Federal University, Chemistry Department, Rostov-On-Don, 344006, Russian Federation.*
[b.] *Kurnakov Institute of General and Inorganic Chemistry of the Russian Academy of Sciences, Moscow, 119991, Russian Federation.*
[c.] *Université Jean Monnet Saint-Etienne, CNRS, Institut d Optique Graduate School, Laboratoire Hubert Curien UMR 5516, 42023, Saint-Étienne, France*
[d.] *Institute of Physical and Organic Chemistry, Southern Federal University, 194/2 Stachka Ave., Rostov-On-Don, 344090, Russia*
[e.] *National Research Center "Kurchatov Institute", Moscow, 123182, Russian Federation.*

Synthesis and characterization of {[MnL_3]Mn[MnL_3]} (1).

0.801 g (3mmol) of 3,5-di-tert-butyl-1,2-benzoquinone-1-monooxime was mixed with 0.362 g (1 mmol) of $Mn(ClO_4)_2 \cdot 6H_2O$ in 5 ml of *iso*-propanol. The solution was sealed inside glass ampoule and heated to 80℃ for 2 days. After slow cooling, ampoule was opened and formed dark olive black crystals of **1** were filtered out and dried in air; the yield was 0.190 g (36.33%), m.p. >300℃.

CAUTION!: although no problems were encountered in this work, care should be taken when using the potentially explosive perchlorate anion (ClO_4^-) containing compounds.

Anal. Calcd for $C_{84}H_{120}N_6O_{12}Mn_3$: C, 64.24%; H, 7.65%; N, 5.35%; O, 12.24%; Mn, 10.52%. Found: C, 64,0 %; H, 7,59%; N, 5,41%.

IR (cm^{-1}): 2952 (w), 2905 (w), 2867 (w), 1536(w), 1479(w), 1461(w), 1359 (w), 1341(w), 1308(w), 1282 (w), 1252(w), 1222 (w), 1196(w), 1120 (s), 1101 (s), 1023 (w), 977 (w), 907(w), 820(w), 765 (w), 639(w), 611 (m), 528 (w), 500(w), 439(w); (see Figure S1B).

UV/vis ($CDCl_3$, nm): 1158; 663; 495; 366 (see Figure S1A).

Complex **1** is soluble in chloroform, methylene chloride, toluene and hardly soluble in ethanol, methanol, acetonitrile and DMSO.

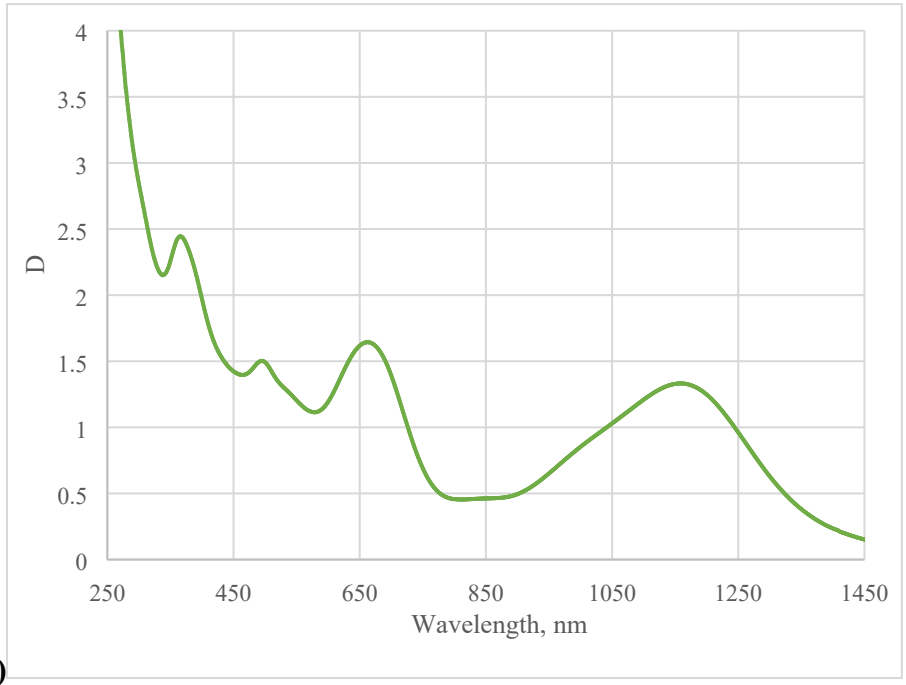

A)

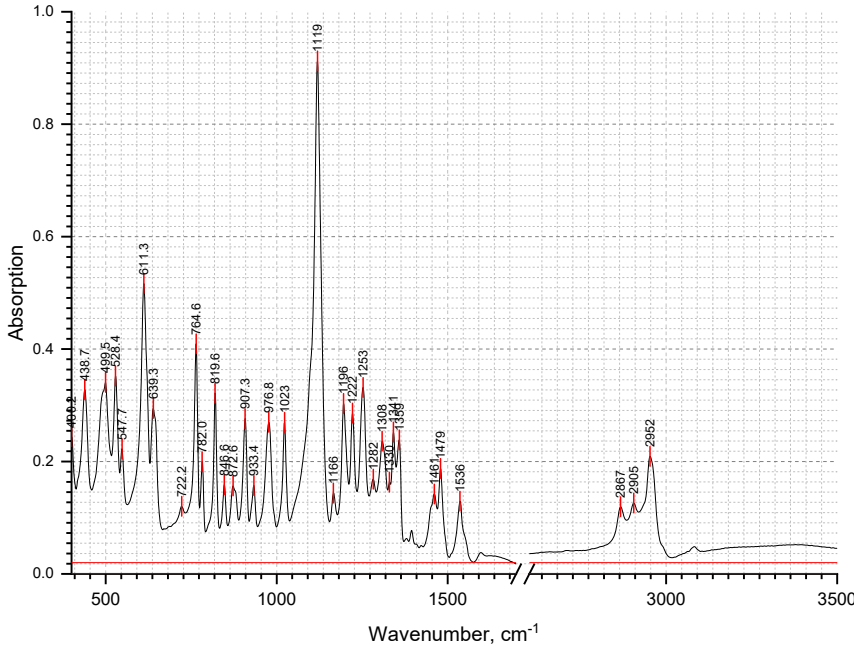

B)

Figure S1. A) UV/vis spectrum of **1** in chloroform solution (C = $1 \cdot 10^{-4}$ M); B) IR spectrum of **1.**

Magnetic susceptibility measurements have been performed using a Quantum Design PPMS-9 susceptometer. DC magnetic susceptibility measurements for 1 have been performed at the 5000 Oe magnetic field in the 2–300 K temperature range. For Ac susceptibility measurements of all the samples, oscillating ac magnetic fields of 5, 3, and 1 Oe within frequency ranges 10–100, 100–1000, and 1000–10000 Hz, respectively, have been applied. All the magnetic measurements were performed on polycrystalline samples sealed in polyethylene bags and covered with mineral oil to prevent the field-induced orientation of crystallites. The paramagnetic components of the magnetic susceptibility χ were determined considering both the diamagnetic contribution evaluated from

Pascal's constants and the contributions of the sample holder and mineral oil. Temperature dependence of magnetic susceptibility and field dependency of magnetization were fitted by PHI program [1]

Computational methods

The quantum-chemical calculations were carried out within density functional theory (DFT) employing the hybrid exchange-correlation functional PBE0[2] and split-valence basis set extended with polarization functions on all atoms 6-311G(d). The Gaussian'09 program was used[3] for calculations. Atomic coordinates of **1** were taken from single crystal X-ray diffraction experiment (SCXRD). For calculations of monomeric anionic unit $[MnL_3]^-$ atomic coordinates were extracted mechanistically from SCXRD data. Energies of different spin states were obtained within unrestricted Kohn-Sham scheme. For data preparation, graphics presentation and visualization of calculation results the Chemcraft program was utilized[4].

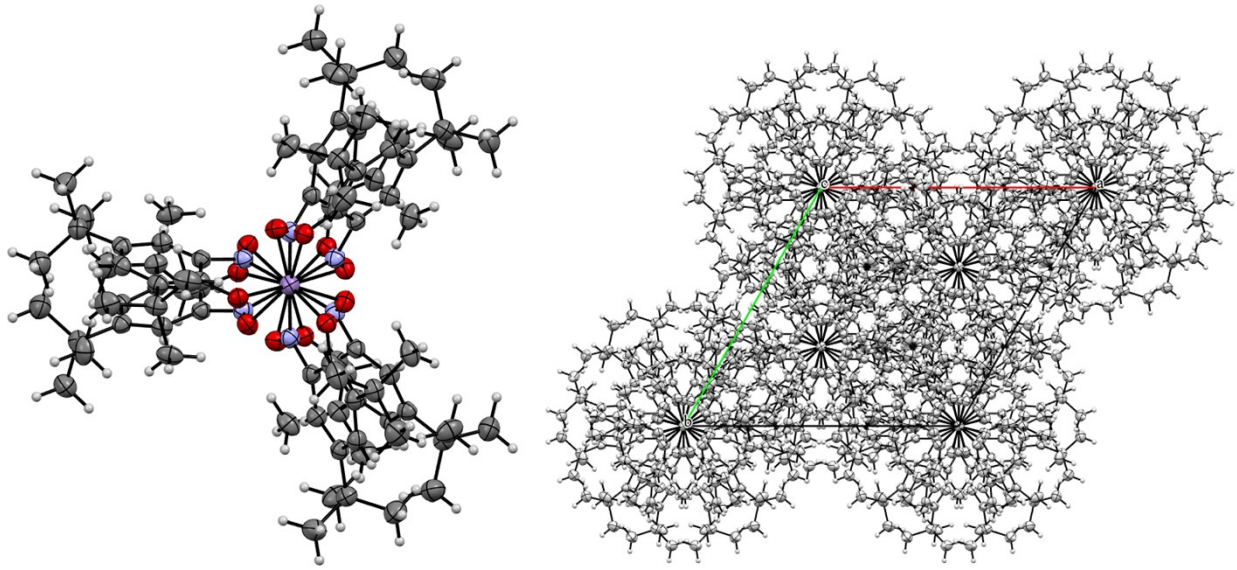

Figure S2. View of the **1** molecule along C_3 proper rotation symmetry axis (left figure, red atoms – oxygen, blue – nitrogen, magenta - manganese). Fragment of the crystal packing of **1** viewed along *c* crystallographic axis (right figure).

Single crystal X-ray diffraction study (SCXRD) of 1

The single crystal X-ray diffraction data sets for sample of **1** were collected at the "Belok/XSA" beamline [5,6] of the Kurchatov synchrotron radiation source (National Research Centre "Kurchatov Institute") equipped with a Rayonix SX165 CCD detector (λ = 0.79475 Å, φ-scanning technique with a step of 1°) in direct geometry (θ = 0°).

The structures were solved by direct methods and refined by the full-matrix least-squares with anisotropic displacement parameters for all nonhydrogen atoms. Hydrogen atoms were positioned

geometrically and refined using a riding model. The calculations were performed with the SHELX–2014/2016 program package [7] *via* OLEX2 1.3 graphical user interface [8].

Table S1. Crystallographic data and the structure refinement statistics for compound **1.**

Parameter	1
Empirical formula	$C_{84}H_{120}Mn_3N_6O_{12}$
Molecular weight, g/mol	1570.67
T, K	100(2)
Crystal system	Trigonal
Space group	*R -3c*
a, Å	16.670(2)
b, Å	16.670(2)
c, Å	53.676(11)
α, deg	90
β, deg	90
γ, deg	120
V, Å^3	12918(4)
Z	6
ρ(calc.), g cm^{-3}	1.211
μ, mm^{-3}	0.572
θ_{min}–θ_{max}, deg	2.2–31.0
F(0 0 0)	5022
Number of measured reflections	26025
Number of independent reflections	3845
R_{int}	0.129
Number of reflections with $I > 2\sigma(I)$	2153
GOOF	1.050
R_1, wR_2 ($I > 2\sigma(I)$)	0.0601, 0.1312
R_1, wR_2 (all data)	0.1212, 0.1586
Residual electron density ($\Delta\rho_{min}/\Delta\rho_{max}$), *e*/Å^3	-0.34/0.36
T_{min}/T_{max}	0.972/0.989
CCDC deposition number	2284760

Table S2. Selected structural parameters for compound **1** {[MnL_3]Mn[MnL_3]}. Atomic numbers are shown in Figure 1.

Parameter	Value	Parameter	Value	Parameter	Value
Bond lengths, Å					
Mn1-O1	1.941(3)	O2-N1	1.297(3)	C2-C3	1.411(5)
Mn1-N1	1.912(3)	N1-C2	1.363(5)	C3-C4	1.358(5)
Mn2-O2	2.138(2)	C1-C2	1.414(4)	C4-C9	1.443(4)
O1-C1	1.300(4)	C1-C10	1.435(5)	C9-C10	1.374(5)
Bond angles, deg					
O1-Mn1-N1	81.64(11)	Mn1-O1-C1	113.73(19)	O2-Mn2-O2_a	87.26(10)
O1-Mn1-O1_a	89.01(11)	Mn1-N1-O2	126.6(2)	O2-Mn2-O2_b	87.25(9)
O1-Mn1-N1_a	166.43(11)	Mn1-N1-C2	115.16(18)	O2-Mn2-O2_c	80.58(9)
O1-Mn1-N1_b	100.58(12)	O2-N1-C2	118.0(3)	O2-Mn2-O2_d	159.00(10)
N1-Mn1-N1_a	90.39(13)	O1-C1-C2	117.2(3)	O2-Mn2-O2_e	109.02(11)
N1_a-Mn1-N1_b	90.39(13)	N1-C2-C1	111.9(3)	Mn2-O2-N1	117.29(19)

Symmetry codes: a: 1-y, x-y, z; b: 1-x+y, 1-x, z ; c: 1/3+y, -1/3+x, 7/6-z ;
d : 4/3-x, 2/3-x+y, 7/6-z; e : 1/3+x-y, 2/3-y, 7/6-z.

Table S3. Continuous symmetry measures OC-6 and TPR-6 calculated for terminal (Mn1 and Mn1') and middle (Mn2) coordination polyhedra with the help of SHAPE 2.1[9] program.

Metal centre	OC-6	TPR-6
Mn1 (Mn1')	3.531	9.373
Mn2	1.398	5.468

Table S4. Bond Valence Sum (BVS) analysis for terminal (Mn1 and Mn1') and middle (Mn2) manganese ions (calculated with PLATON [10, 11] program).

Ion	Mn1(Mn1')				Mn2			
Assumed valence	1	2	3	4	1	2	3	4
BVS	1.067	4.525	4.289	4.157	0.623	2.342	2.160	2.120
Diff*	**0.067**	2.525	1.289	0.157	0.377	**0.342**	0.84	1.880

* Diff = abs(BVS-assumed valence)

Table S5. Bond length's distribution in the $\mathbf{L}^{-}$ ligand of **1** compared to average bond lengths (Å) for C–C, C–N, and C–O bonds of metal N-arylamidophenoxides and catecholates as a function of ligand oxidation state (taken from [12]). r – Correlation coefficient between corresponding line (bond lengths in specific oxidation state) and data for compound **1.**

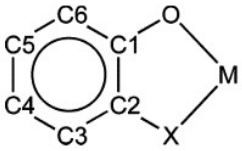

Bond	C-O	C-N	C1-C2	C2-C3	C3-C4	C4-C5	C5-C6	C6-C1	r
Compound **1**	1.300	1.363	1.414	1.411	1.358	1.443	1.373	1.435	
Ligand oxidation state [a]									
-2 (21)	1.364	1.402	1.411	1.389	1.395	1.391	1.401	1.399	0.58
-1.5 (7)	1.337	1.377	1.422	1.401	1.388	1.404	1.395	1.410	0.90
-1 (73)	1.302	1.348	1.444	1.418	1.368	1.429	1.376	1.427	0.95
0 (8)	1.238	1.298	1.511	1.431	1.347	1.468	1.352	1.455	0.93

[a] In brackets number of the structures used for averaging[12] are shown

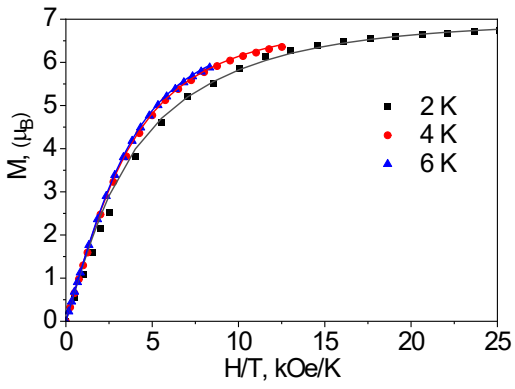

a)

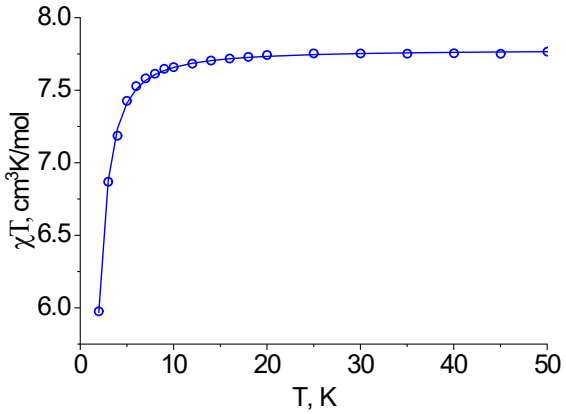

b)

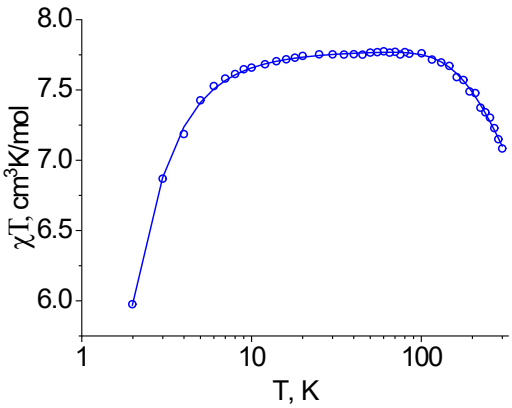

c)

Figure S3. – a) The reduced magnetization of **1** measured at 2, 4 and 6 K; b) χT product *vs* T in low temperature range 0 - 50 K; c) χT product *vs* T in logarithmic scale. Symbols represent experimental points; solid lines correspond to the best-fit curves.

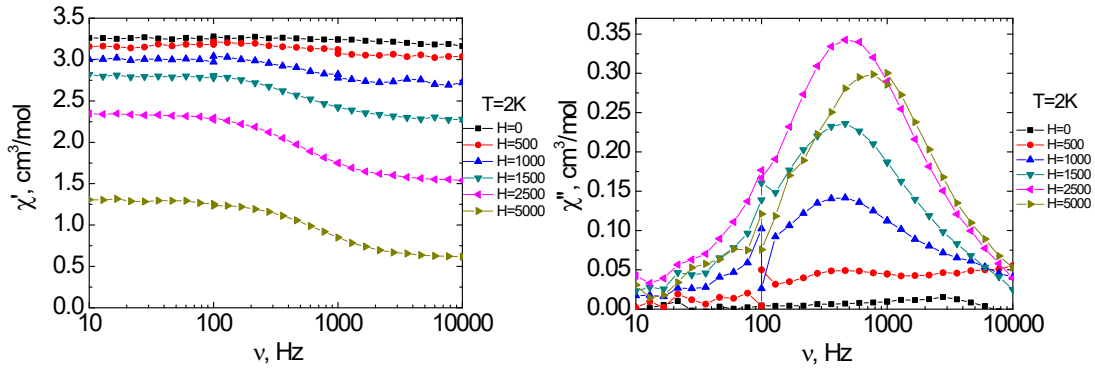

Figure S4. – Frequency dependencies of real (χ', left) and imaginary (χ'', right) parts of dynamic magnetic susceptibility of **1** at different external supporting magnetic field at T = 2 K. Solid lines are drawn for clarity.

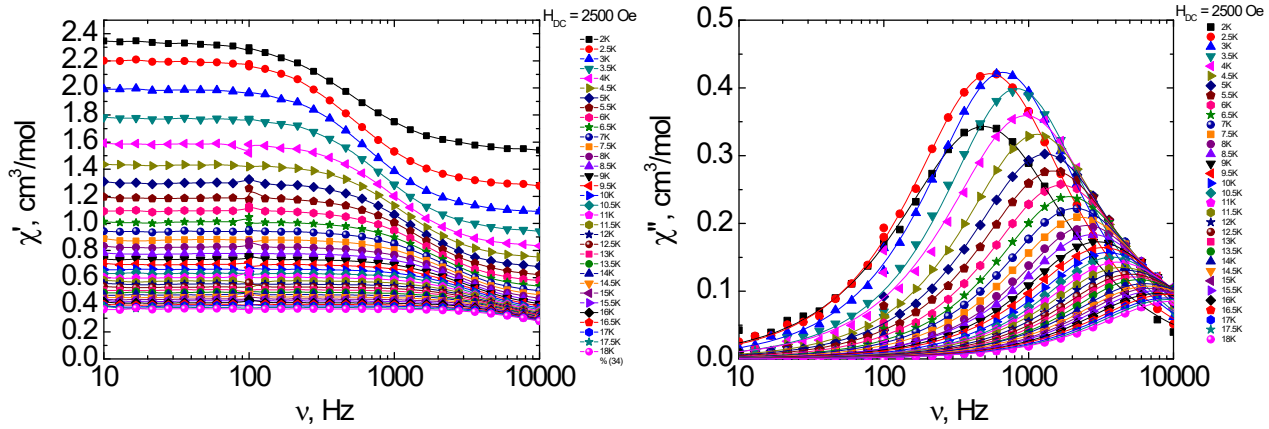

Figure S5. – Frequency dependencies of real (χ', left) and imaginary (χ'', right) parts of dynamic magnetic susceptibility of **1** in the 2-18 K temperature range at external dc magnetic field of 2500 Oe. Solid lines show approximations of the experimental data with generalized Debye model.

References

1. N. F. Chilton, R. P. Anderson, L. D. Turner, A. Soncini and K. S. Murray, *J. Comput. Chem.*, 2013, **34**, 1164-1175.
2. M. Ernzerhof and J. P. Perdew, *J. Chem. Phys.*, 1998, **109**, 3313-3320.
3. M. J. Frisch, G. W. Trucks, H. B. Schlegel, G. E. Scuseria, M. A. Robb, J. R. Cheeseman, V. B. G. Scalmani, B. Mennucci, G. A. Petersson, H. Nakatsuji, M. Caricato, X. Li, H. P. Hratchian, A. F. Izmaylov, J. Bloino, G. Zheng, J. L. Sonnenberg, M. Hada, M. Ehara, K. Toyota, R. Fukuda, J. Hasegawa, M. Ishida, T. Nakajima, and O. K. Y. Honda, H. Nakai, T. Vreven, J. A. Montgomery, Jr., J. E. Peralta, F. Ogliaro, M. Bearpark, J. J. Heyd, E. Brothers, K. N. Kudin, V. N. Staroverov, R. Kobayashi, J. Normand, K. Raghavachari, A. Rendell, J. C. Burant, S. S. Iyengar, J. Tomasi, M. Cossi, N. Rega, J. M. Millam, M. Klene, J. E. Knox, J. B. Cross, V. Bakken, C. Adamo, J. Jaramillo, R. Gomperts, R. E. Stratmann, O. Yazyev, A. J. Austin, R. Cammi, C. Pomelli, J. W. Ochterski, R. L. Martin, K. Morokuma, V. G. Zakrzewski, G. A. Voth, P. Salvador, J. J. Dannenberg, S. Dapprich, A. D. Daniels, O. Farkas, J. B. Foresman, J. V. Ortiz, J. Cioslowski, and D. J. Fox, Gaussian 09, Revision A.02, 2009.

4. G. A. Zhurko, Chemcraft ver. 1.6, build 332, http://www.chemcraftprog.com, 2010.
5. V. A. Lazarenko, P. V. Dorovatovskii, Y. V. Zubavichus, A. S. Burlov, Y. V. Koshchienko, V. G. Vlasenko and V. N. Khrustalev, *Crystals*, 2017, **7**.
6. R. D. Svetogorov, P. V. Dorovatovskii and V. A. Lazarenko, *Cryst. Res. Technol.*, 2020, **55**, 1900184.
7. G. Sheldrick, *Acta Crystallogr. Sect. A:*, 2015, **71**, 3-8.
8. O. V. Dolomanov, L. J. Bourhis, R. J. Gildea, J. A. K. Howard and H. Puschmann, *J. Appl. Crystallogr.*, 2009, **42**, 339-341.
9. M. Llunell, D. Casanova, J. Cirera, P. Alemany and S. Alvarez, SHAPE (2.1); Universitat de Barcelona: Barcelona, Spain, 2013.
10. A. Spek, *J. Appl. Crystallogr.*, 2003, **36**, 7-13.
11. A. Spek, *Acta Crystallogr. Sect. D*, 2009, **65**, 148-155.
12. S. N. Brown, *Inorg. Chem.*, 2012, **51**, 1251-1260.